Pneumothorax Lung Disease Segmentation: A Deep Learning Approach

Albert Millan
Department of Computer Science
Tsinghua University
Beijing 100084, P. R. China
millanta10@mails.tsinghua.edu.cn

Bastien Bedu
Department of Computer Science
Tsinghua University
Beijing 100084, P. R. China
bda19@mails.tsinghua.edu.cn

Henry Xiang
Department of Computer Science
Tsinghua University
Beijing 100084, P. R. China
xiangmr9@mails.tsinghua.edu.cn

Abstract

Pneumothorax is a severe, and sometimes life threatening condition that occurs when air leaks into the space between the lung and the chest wall, compressing the lung and causing it to collapse. This paper aims to address the problem by presenting a deep learning model, involving UNet++ and EfficientNet, to identify and segment pneumothorax from a dataset consisting of patients' lung radiographies. We report a 0.8368 dice competition, 124^{th} out of 350 in the kaggle ranking.

1 Introduction

Pneumothorax is a severe, and sometimes life threatening condition that occurs when air leaks into the space between the lung and the chest wall, compressing the lung and causing it to collapse. It is often characterized by a sharp, sudden chest pain, and shortness of breath (1). Within the United States it is estimated to occur 7.4 - 18.0 times per 100,000 males, and 1.2 - 6.0 times per 100,000 females. While the mortality rate is low, the recurrence rate for the condition is 14-30% over 3 years (2), and pneumothorax remains a health condition with severe symptoms that is reliant on prompt diagnosis, and proper treatment.

1.1 Motivation

Timely review of radiographs is paramount for the treatment of pneumothorax (3). However, automated medical image segmentation is currently no simple task due to a large variation in quality among medical imaging equipment. This, combined with the manual nature of doctors checking radiographs to make diagnoses, is a process that can certainly be improved upon. The development of an AI system that can accurately identify the presence, extent and location of pneumothorax within a radiograph image would considerably aid doctors in a variety of clinical situations. For example, AI can be used to triage chest x-rays for priority interpretation (3), as well as work alongside doctors to aid them in confirming their own diagnoses and interpretations of x-rays. We hope this AI can make diagnoses more accurate and efficient, as AI in medical imaging continues to advance and save lives.

Preprint. Under review.

1.2 Aim

This paper describes the theoretical foundation required to implement an algorithm that can efficiently ***identify*** and ***localize*** pneumothorax within a set of patients' images data. The former task, identification, aims to correctly classify pneumothorax within the patients' images. The latter task, localization, outlines to the nearest pixel the region from an image where pneumothorax is located. Evaluation of the model therefore considers its ability to perform both tasks. The authors are considering, however, using two distinct models, one for each task, as an optimal solution to maximize the predictive performance.

The model has been trained using a private dataset provided for the kaggle competition by the *Society for Imaging Informatics in Medicine* (4). The training dataset consists of 12,955 lung radiographies such as the one shown in figure 1. The given test dataset consists of 3,205 images. An unknown number of test sample images are also inputted to the model upon uploading on kaggle, acting as a validation set. Medical images are encoded under DICOM format, containing an uncertain number of annotations, as well as an ID and a run-length-encoded (RLE) masks, further explained in section 3.1. The images are initially decoded and subsequently inputted into the model. The model then determines whether pneumothorax is present. Should this be the case, it proceeds to estimate the region within the image where it is located. Results are then compared to those provided by the kaggle competition ranking as well as related projects from other academics.

Figure 1: Caption

The paper is structured in the following manner. Section 2 is literature research, which consists of a discussion of similar solutions and approaches that have been implemented in the past for solving this problem, and the conclusions drawn from them. Section 3.1 provides an explanation of the data set used in this project, for both training and testing of the algorithms used, while section 3.3 goes more in-depth on said algorithms. Section 4.0.1 consists of an explanation of the evaluation metric, and section **??** of a comparison of our results to past results obtained by others. Finally, section 5 will be a discussion of the final conclusion based on the obtained results.

2 Literature Research

Past research and advances made pertaining the field of medical image analysis and segmentation is rich within the literature. A significant volume of solutions have been proposed, with topics ranging across a variety of fields including brain (5), pancreatic (6), lung (7) tumor or echocardiogram pattern (8) segmentation amongst others. While several distinct algorithmic models have been tested, the convolutional neural network (CNN) or variants of this model have shown to yield state-of-the-art predictive accuracy (9). Due to the similarity of such approaches to pneumothorax segmentation problem, we present an analysis of the related problems and algorithmic solutions.

The comparison and identification of deep learning models to solve a given problem is a widely used methodology to filter out the superior model. Desphande et. al(10) implemented and contrasted three distinct deep learning models, namely (1) CNN, (2) fully convolutional neural network (FCN) and (3) multiple-instance learning (MIL) model. The FCN aimed to provide more information on the location of the presence of pneumothorax than the traditional CNN approach, at the expense of classification accuracy, whereas the multiple-instance learning model intended to provide a middle-ground solution for classification accuracy and location detection that lies between the CNN and FCN approaches. The results show that the CNN exhibited superior ability to identify pneumothorax, notwithstanding,

the FCN more reliably localized the condition within the testing images. Furthermore, the MIL outperformed the FCN in the pneumothorax identification task while also providing information on the general locations of where pneumothorax is predicted to be present (10).

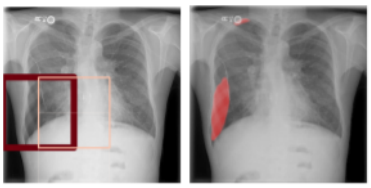

(c) MIL (d) FCN

Figure 2: MIL vs. FCN Pneumothorax Segmentation

Support vector machines (SVM) have also been utilized for x-ray image analysis, specifically to detecting pneumothorax. Research performed by Yuan-Hao Chan et. al, for example, showed an application of SVM in order to classify images. SVM was utilized, along with local binary pattern (LBP) to achieve an 85 percent accuracy rate. Author used ULBP in order to extract features from the x-ray images, which were then utilized by SVM to train and classify lung images. (11)

In general, both deep and machine learning techniques have shown promising results when applied to detecting pneumothorax via radiographs, and seem to be on their way towards assisting doctors with image/patient prioritization, speeding up diagnoses, and increasing efficiency in an otherwise very manual process.

3 Methodology

3.1 Dataset Explanation

The provided dataset contains two separate sets of data for each instance/element. On one hand, the chest x-ray image is encoded following the DICOM format. The DICOM format is an encoding used for medical data, storing information such as the patient's gender, age or name, as well as the media files. In this case, the file of interest for the model is the chest x-ray image. On the other hand, there is an encoded array of pixels defining the location and contour of the detected pneumothorax. This encoded array of pixels is a mask of the DICOM image, and is known as Run-Length-Encoding (RLE). For illustration purposes we show a simple example in figure 3.1, while an example from the dataset is provided in 4. Note that we are using a relative form of RLE. If no collapsed lung is found, then the mask is set to -1.

```
-----  5 pixels
-----  5 pixels
--xxx  2 pixels, 3 pixels with mask
---xx  3 pixels, 2 pixels with mask
-----  5 pixels
```

Figure 3: The mask *12,3,3,2,5* on a $5x5$ image indicates that there are 12 pixels without mask, followed by 3 pixels with the mask, 3 without, etc.

```
1.2.276.0.7230010.3.1.4.8323329.14508.1517875252.443873,387620 23 996 33 986 43 977 51 968 58 962 65
956 70 952 74 949 76 946 79
```

Figure 4: Example of a mask from the training dataset.

The training set consists of around 12000 images, all of which are rescaled to 256 pixels for the purposes of training. Within this set of 12000 images, 90% is used for training, and 10% is allocated for the validation set. Finally, 3225 images compose the test set.

3.2 Data Pruning

Data augmentation was performed during the training process. The operations involved include random contrast, brightness and gamma, followed by elastic transform and grid and optimal distortion, as well as flips and crops. The first three three operations modify the light distribution throughout the images. The following three alter the shape of the object within the images. These operations are shown in figure 5.

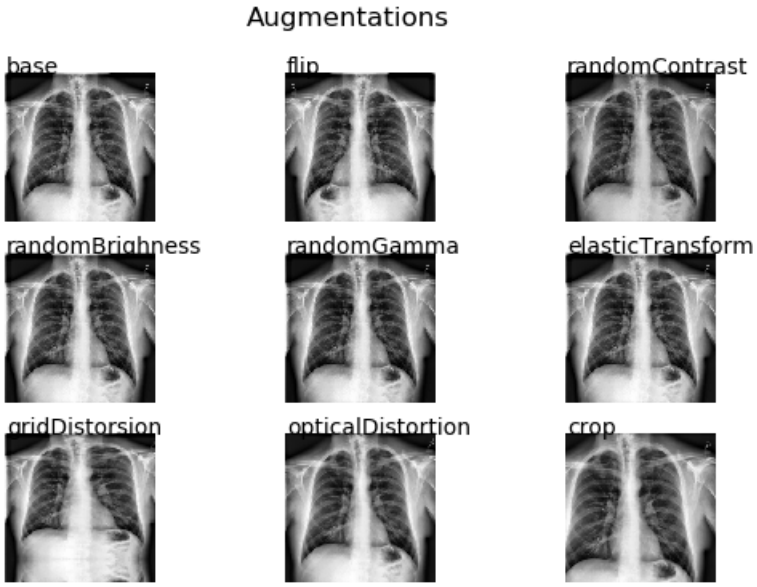

Figure 5: Data Augmentation

On each training iteration, a given image is subject to an augmentation operation based on a probability distribution. This way, certain augmentation operations are prioritized. The purpose is to expose the model to a larger and more varied set of new data. Multiple augmentations may be applied to a single image simultaneously to generate an augmented image.

3.3 Algorithm Explanation

The model employed for this task is the UNet (12). UNet uses a rather novel loss weighting scheme for each pixel such that there is a higher weight at the border of segmented objects. The main idea is to supplement a usual contracting network by successive layers, where pooling operators are replaced by up-sampling operators. The proposed structured for the model aims to address two primary operations, namely down-sampling and up-sampling. The down-sampling phase aids the model to capture the intrinsic properties of the images. The up-sampling phase utilizes the aforementioned properties in order to identify the portions of the images which correspond to lung-segmentation.

The down-sampling phase aids the model to capture the intrinsic properties of the images. Up-sampling phase that utilizes the aforementioned properties in order to identify the portions of the images which correspond to lung-segmentation.

The model was further improved by introducing intermediate layers to skip connections of the UNet. The proposed improvement naturally forms multiple new up-sampling paths from different depths. This results in far better performance than a traditional UNet. This approach is formally referred to as UNet++ (13), and is depicted in figure 6.

The down sampling procedure was performed using EfficientNet (14), with weights pre-trained on imagenet.

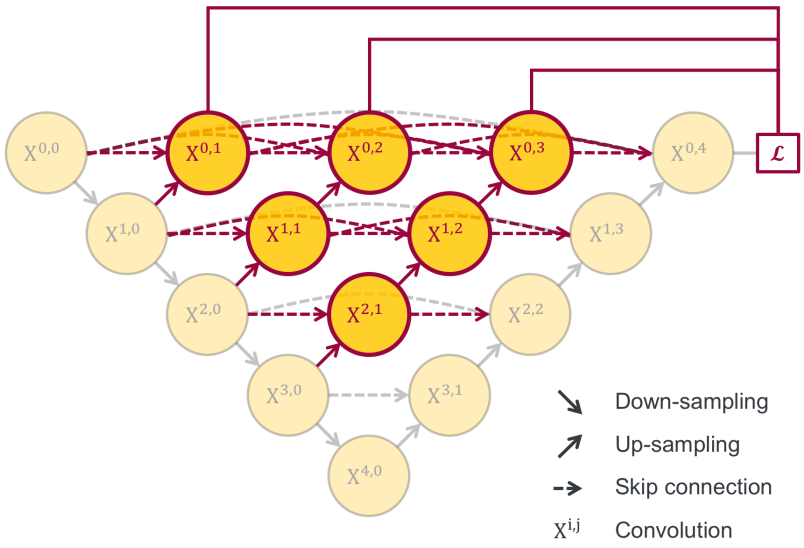

Figure 6: Representation of UNet++ model employed.

3.3.1 Training Conditions

The proposed model was trained on the allocated AWS cloud computing server using a Tesla K80 GPU. The aforementioned computing device had severe memory restrictions. Consequently, the maximum batch-size employed was limited to 12 images, even after down-sizing the image to 256x256. The server also had time limitations, so maximum training time allowed was 12 hours. In turn, only 33 epochs were permitted. Train test ration was 90-10%, the recommended based on the kaggle project guidelines. The derived threshold (see section 4). The training conditions are illustrated in table 1.

Epochs	Batch Size	Image Size	Threshold	Train Test Split
33	12	256x256	0.75	90:10

Table 1: Training Conditions

4 Results

The model's output contains images of similar size to the training data. Each pixel on any given image contains a floating value between 0 and 1. A larger value represents a greater likelihood that pneumothorax is present. We then define a threshold, used in conjunction with the aforementioned values in order to locate areas affected by pneumothorax. Any pixel beyond the defined threshold indicates the presence of pneumothorax.

The dice coefficient was used to evaluate the effectiveness of the model, yielding a score of 0.8368. There is still room for improvement, considering the top score is 0.8679. A summary of the performance of our model relative to that of competitors is table 2.

Competition	**Dice Coefficient**
Aimolding Anuar	0.8679
Vasiliy Kotov	0.8537
Unet++ & EfficientNet	0.8368
Mobassir	0.8353

Table 2: Kaggle competition result comparison.

4.0.1 Evaluation Metric

The scoring system uses the dice coefficient. This metric will produce a floating number between 0 and 1. A coefficient of **1** indicates a perfect match on the predicted pneumothorax maligned areas with the actual pneumothorax affected lungs given via the data set. Meanwhile, a coefficient of **0** indicates that no single pixel of pneumothorax was correctly predicted by the algorithm. This coefficient is computed using the formula below:

$$\frac{2 * |X \cap Y}{|X| + |Y|} \tag{1}$$

In this formula, ***X*** is the set of pixels predicted as the pneumothorax affected area, and ***Y*** is the set of pixels representing the pneumothorax affected areas defined by the actual data set. The final score is the mean of the Dice coefficients for each image in the test set.

5 Conclusion

This paper presented a method for automated pneumothorax detection. We proposed a combination of models involving UNet++ and EfficientNet. Despite the severe limitations in terms of computing power and server access time, this solution achieved optimal performance. While the model effectively identifies pneumothorax within images, it still struggles to precisely detect the location of the disease. Further improvements are required to enhance the overall performance of the model. Overall, this solution shows promise towards becoming a practical solution in the healthcare industry in the context of improving diagnosis times and quality of care for patients with pneumothorax.

Acknowledgments

This project was developed for the course Advanced Machine Learning at Tsinghua University.

References

[1] 2019.

[2] J. Custombrado and S. Ghassemzadeh, *Pneumothorax, Spontaneous*. StatPearls Publishing LLC, 2018.

[3] `https://www.kaggle.com/c/siim-acr-pneumothorax-segmentation`, 2019.

[4] `https://siim.org/`, 2019.

[5] Z. Sobhaninia, S. Rezaei, A. Noroozi, M. Ahmadi, H. Zarrabi, N. Karimi, A. Emami, and S. Samavi, "Brain tumor segmentation using deep learning by type specific sorting of images," *CoRR*, vol. abs/1809.07786, 2018.

[6] S. Hussein, P. Kandel, C. W. Bolan, M. B. Wallace, and U. Bagci, "Lung and pancreatic tumor characterization in the deep learning era: Novel supervised and unsupervised learning approaches," *IEEE Transactions on Medical Imaging*, vol. 38, pp. 1777–1787, Aug 2019.

[7] M. Anthimopoulos, S. Christodoulidis, L. Ebner, A. Christe, and S. Mougiakakou, "Lung pattern classification for interstitial lung diseases using a deep convolutional neural network," *IEEE Transactions on Medical Imaging*, vol. 35, pp. 1207–1216, May 2016.

[8] S. Leclerc, E. Smistad, J. Pedrosa, A. Østvik, F. Cervenansky, F. Espinosa, T. Espeland, E. A. R. Berg, P. Jodoin, T. Grenier, C. Lartizien, J. D'hooge, L. Lovstakken, and O. Bernard, "Deep learning for segmentation using an open large-scale dataset in 2d echocardiography," *IEEE Transactions on Medical Imaging*, vol. 38, pp. 2198–2210, Sep. 2019.

[9] H. Shin, H. R. Roth, M. Gao, L. Lu, Z. Xu, I. Nogues, J. Yao, D. Mollura, and R. M. Summers, "Deep convolutional neural networks for computer-aided detection: Cnn architectures, dataset characteristics and transfer learning," *IEEE Transactions on Medical Imaging*, vol. 35, pp. 1285–1298, May 2016.

[10] A. Gooßen, H. Deshpande, T. Harder, E. Schwab, I. Baltruschat, T. Mabotuwana, N. Cross, and A. Saalbach, "Pneumothorax detection and localization in chest radiographs: A comparison of deep learning approaches," *MIDL*, vol. abs/1907.07324, 2019.

[11] Y.-H. Chan, Y.-Z. Zhen, H.-C. Wu, M.-C. Wu, and H.-M. Sun, "Effective pneumothorax detection for chest x-ray images using local binary pattern and support vector machine," *Journal of Healthcare Engineering*, 2018.

[12] O. Ronneberger, P. Fischer, and T. Brox, "U-net: Convolutional networks for biomedical image segmentation," *CoRR*, vol. abs/1505.04597, 2015.

[13] Z. Zhou, M. M. R. Siddiquee, N. Tajbakhsh, and J. Liang, "Unet++: A nested u-net architecture for medical image segmentation," *CoRR*, vol. abs/1807.10165, 2018.

[14] M. Tan and Q. V. Le, "Efficientnet: Rethinking model scaling for convolutional neural networks," *CoRR*, vol. abs/1905.11946, 2019.